

The Development of Scotopic Sensitivity

Anne B. Fulton and Ronald M. Hansen

PURPOSE. Test the hypothesis that the developmental increases in rod photoreceptor sensitivity and rod-mediated visual sensitivity at 10°, 20°, and 30° eccentric are concurrent. It is known that maturation of the parafoveal (10° eccentric) rod outer segments and visual sensitivity is delayed compared to that at 30° eccentric.

METHODS. Rod isolated electroretinographic (ERG) responses to full-field stimuli were obtained from dark-adapted subjects ($n = 71$), ranging in age from early infancy through middle age. Rod photoreceptor sensitivity was calculated by fitting a model of the activation of phototransduction to the a-wave response. Rod driven b-wave sensitivity was calculated from stimulus-response functions. A logistic growth model was used to summarize the developmental increases in sensitivity of the rod photoreceptors and the b-wave. Previously reported dark-adapted, rod-mediated visual sensitivities at 10°, 20°, and 30° eccentric, obtained using preferential looking procedures, were reanalyzed using the logistic growth model.

RESULTS. The logistic growth model accounted for 57% to 85% of the variance of each sensitivity parameter with age in normal subjects. The shape of the growth curve and the age at which sensitivity reaches 50% of the adult value is similar (10.0–13.5 weeks) for the rods, the b-wave, and peripheral visual sensitivity, but is significantly older, 19.5 weeks, for rod-mediated parafoveal visual sensitivity.

CONCLUSIONS. Rod photoreceptor sensitivity and peripheral, rod-mediated visual sensitivity develop concurrently. A parsimonious explanation is that rod photoreceptor sensitivity determines dark-adapted, rod-mediated visual sensitivity during development. (*Invest Ophthalmol Vis Sci.* 2000;41:1588–1596)

The dark-adapted, rod-mediated visual sensitivity of young infants, according to most published data, is more than a log unit below that of adults. For instance, at ages 8 to 12 weeks, dark-adapted visual sensitivities, estimated using two alternative, forced-choice preferential looking procedures, are 1.1 to 1.7 log units lower than those of adults.^{1–5} Over the same limited age range in early infancy, sensitivities derived from the electroretinographic (ERG) a- and b-waves are barely half a log unit less than that of adults.^{4,6,7} The course of maturation of rod-mediated visual sensitivity, however, depends on the retinal region tested. The development of parafoveal (10° eccentric) sensitivity^{8,9} and rod outer segments¹⁰ is delayed compared to that in more peripheral retina. Furthermore, there is only a half log unit discrepancy between peripheral visual sensitivity for detecting 30° eccentric 2° diameter stimuli in 10-week-old and adult individuals.^{8,9} In other words, for some stimulus conditions, the immaturities in ERG and visual sensitivity are the same. The rods are thought to account for immaturities of the ERG a- and b-wave.^{7,11} Thus, despite some evidence to the contrary,^{1,12,13} the immature

rods, which have short outer segments¹⁴ and low rhodopsin content¹⁵ with consequent low probability of photon capture, cannot be dismissed as the primary determinant of infants' low, dark-adapted, rod-mediated visual sensitivity.

In developing mammalian retina, rod outer segments grow longer,^{10,11,16–22} following a course of logistic growth,²³ and finally asymptote at adult length with equal synthesis and disposal of outer segment discs.¹⁸ In rats,^{11,16} logistic growth^{11,19,23} also describes the developmental increase in rhodopsin content (Fig. 1) during outer segment development. The developmental increase in rhodopsin of several species,^{19–22} including human,¹⁵ has also been summarized using a logistic growth model. By using this mathematical model of growth, the courses of development of the visual pigment and retinal responses could be compared.¹¹ The courses of the developmental increase in rat rod photoreceptor and inner retinal sensitivity, derived from the electroretinographic (ERG) a- and b-waves, are indistinguishable from that of rhodopsin.¹¹ That is, according to a logistic growth model, Age₅₀, the age at which a parameter is half the adult value, for rat rhodopsin, rod photoreceptor sensitivity, and b-wave sensitivity do not differ significantly.¹¹

In the present study, we tested the hypothesis that dark-adapted, rod photoreceptor sensitivity predicts dark-adapted, rod-mediated visual sensitivity during infancy. We have used contemporary ERG procedures to assess rod photoreceptor sensitivity, represented by the ERG a-wave,^{24,25} and b-wave sensitivity,²⁶ as well as the developmental increases in the saturated amplitudes of the rod photoreceptor response and rod driven b-wave. Additionally, we have reanalyzed the devel-

From the Department of Ophthalmology, Children's Hospital and Harvard Medical School, Boston, Massachusetts.

Supported in part by Grant R01-EY10597 from the National Institutes of Health, Bethesda, Maryland.

Submitted for publication August 23, 1999; revised December 9, 1999; accepted December 16, 1999.

Commercial relationships policy: N.

Corresponding author: Anne Fulton, Department of Ophthalmology, Children's Hospital and Harvard Medical School, 300 Longwood Avenue, Boston, MA 02115. fulton_a@a1.tch.harvard.edu

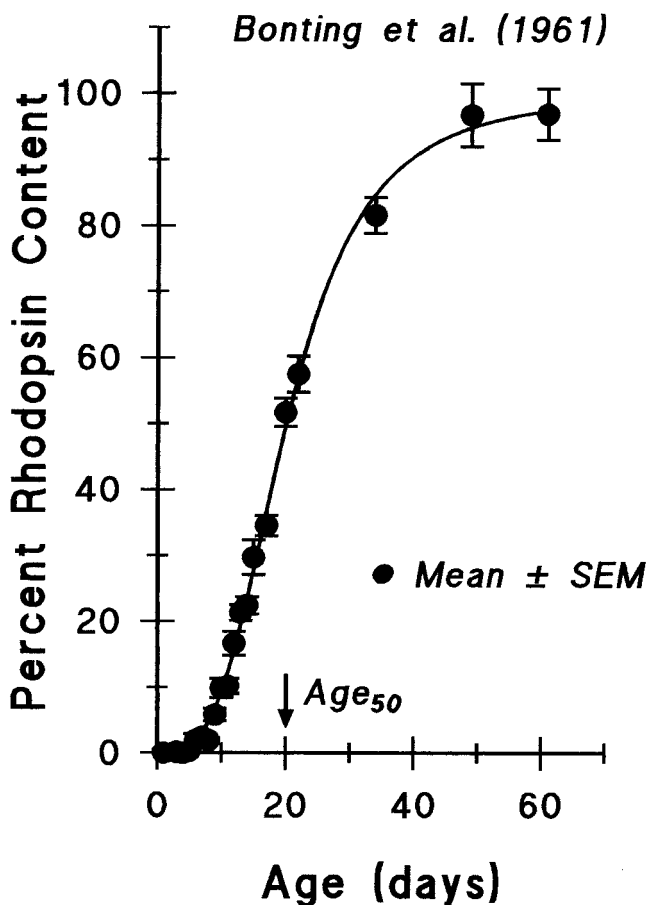


FIGURE 1. The points plot the percent of the mean adult rhodopsin content per eye as a function of age during rat rod photoreceptor development. The data are taken from Table 2 of Bonting et al.¹⁶ The smooth curve is a logistic growth curve of the form $y/y_{\max} = \text{Age}^n / (\text{Age}^n + \text{Age}_{50}^n)$, where Age_{50} is the age at which y is 50% of y_{\max} , the adults' value; the exponent n indicates the steepness of the function about Age_{50} . According to the logistic growth curve fit to the points, Age_{50} is 20 days, and the exponent n is 3.3. The fitted curve accounts for 99% of the variance of rhodopsin with age.

omental increases in dark-adapted, rod-mediated visual sensitivity.^{3,6,8,9,27-30} To facilitate comparison of the course of development of the several response parameters, a logistic growth model is used to summarize the variation of each response parameter with age.

METHODS

ERG Procedures

The left pupil was dilated with cyclopentolate, 1%, and the subject was dark-adapted for 30 minutes. Parents stayed with infants and children throughout the procedure. After dark adaptation, in dim red light, proparacaine, 0.5%, was instilled, and a bipolar Burian-Allen electrode was placed on the left cornea. The ground electrode was placed over the left mastoid.

Blue (Wratten 47B; $\lambda < 510$ nm) strobe stimuli (Novatron, Dallas, TX) were delivered through a 41-cm integrating sphere, controlled in intensity by calibrated neutral-density filters, and

ranged from those that evoked a small b-wave ($< 15 \mu\text{V}$) to those that saturated the a-wave amplitude and slope. Also, stimulus-response functions to red (Wratten 29; $\lambda > 610$ nm) flashes were obtained. To isolate the rod function, the responses to photopically matched red flashes were subtracted digitally from the responses to blue flashes.³¹ The unattenuated flash, measured with a detector (S350; United Detector Technology, Orlando, FL) placed at the position of the subject's cornea, was $3.82 \log \mu\text{W}/\text{cm}^2$ per flash. Retinal illuminance varies directly with pupillary diameter and the transmissivity of the ocular media and inversely with the square of the posterior nodal distance.⁶ The scotopic troland value³² of the stimulus was calculated, taking each subject's pupillary diameter and the average axial length³³ into account.^{3,6} Thus, the maximum intensity blue light produced about $+3.6 \log$ scot td sec retinal illuminance in both infants and adults. If 1 scotopic troland produces ~ 8.5 isomerizations/rod/flash,³⁴ the maximum intensity blue flash produced $\sim 34,000$ isomerizations per rod per flash.

All responses were differentially amplified (bandpass 1-1000 Hz; gain: 1000), displayed on an oscilloscope, digitized, and stored on disc for analysis later. An adjustable voltage window was used to reject records contaminated by artifacts. Two to 16 responses were averaged in each stimulus condition. The interstimulus interval ranged from 2 to 60 seconds and was selected so that subsequent b-wave amplitudes were not attenuated.

The rod photoresponse characteristics were calculated from the a-wave responses using the Hood and Birch²⁴ formulation of the Lamb and Pugh^{25,35} model of the biochemical processes involved in the activation of phototransduction. A curve-fitting routine (MATLAB, fmins) was used to determine the best fitting values of S , a sensitivity parameter, and $R_{\text{mp}3}$, the saturated response amplitude, in

$$R(i, t) = R_{\text{mp}3} (1 - \exp[-0.5S I(t - t_d)^2]), \quad (1)$$

where I is the flash in isomerizations/rod/flash, and t_d is a brief delay. Fitting of the model was restricted to the leading edge of the a-wave response or to a maximum of 20 msec after stimulus onset. All three parameters were free to vary.

For the rod driven b-wave, which represents mainly the activity of the on-bipolar cells,^{26,36} the stimulus-response function

$$V/V_{\max} = I/(I + \sigma) \quad (2)$$

was fit to the b-wave amplitudes of each subject using an iterative procedure that minimized the mean square deviation of the data from the equation. In this Equation 2, V is the b-wave amplitude, V_{\max} the saturated amplitude, I the stimulus in scot td sec, and σ the stimulus that evoked a half-maximum b-wave amplitude. Thus, $1/\sigma$ is a measure of sensitivity. The stimulus-response function was fit up to those higher flash intensities at which a-wave intrusion occurs.³⁷

Subjects

The main data are from 71 normal subjects recruited for study of rod photoreceptor function. Healthy, term-born infants, ages 23 through 100 days ($n = 47$) were recruited by mail. a-Wave

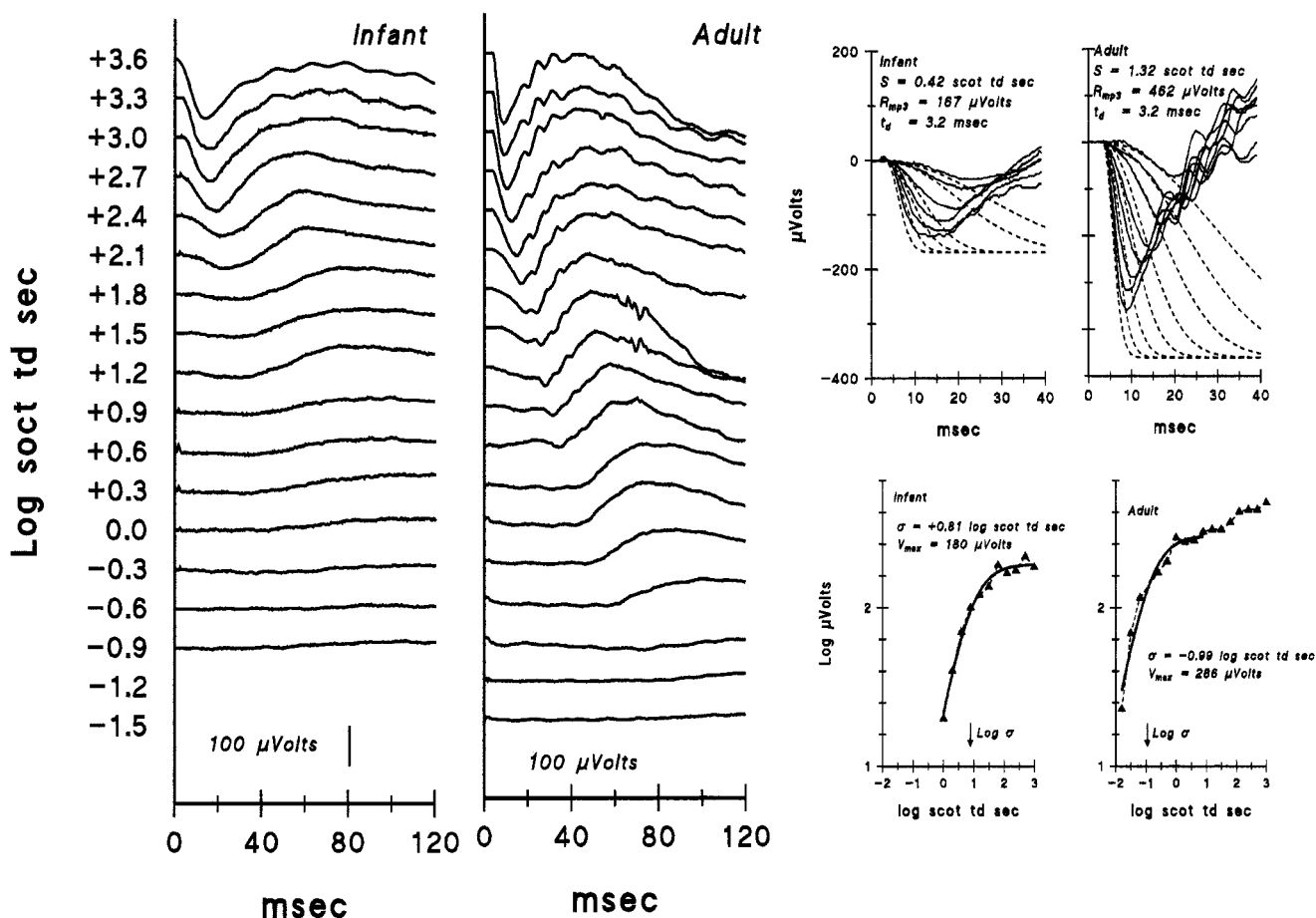


FIGURE 2. Sample ERG records and model fits of a-wave and b-wave responses in a 33-day-old infant and a 35-year-old adult. The numbers to the left of the ERG traces indicate the stimulus in log scot td sec. *Top right:* in these two panels the first 40 msec of the ERG responses are shown by the *continuous lines* and the model (Eq. 1) fit to the a-wave by the *dashed lines*. The calculated values of S , R_{mp3} , and t_d are as indicated. *Bottom right:* in these two panels, the *triangles* plot b-wave amplitude as a function of stimulus intensity. The *smooth curves* represent Equation 2 fit to the points, up to those representing responses to higher intensity stimuli at which the a-wave intrudes.³⁷ The calculated values of σ and V_{max} are as indicated.

data from seven were included in a previous report.⁷ All had been born within 7 days of their due date and were in good general health. Normal child and adult control subjects (ages 8–52 years, $n = 25$) were also recruited; ERG data of 20 of these have been included as control data in a clinical report.³⁸ No subject had a family history of eye or vision problems. Thorough ophthalmic examination disclosed no abnormalities. Written, informed consent was obtained from adult subjects and the parents of the infants and children. This study conformed to the tenets of the Declaration of Helsinki and was approved by the Children's Hospital Committee on Clinical Investigation.

The subjects described included few children. To obtain ERG data from children, we reviewed our clinical ERG database listing 1164 patients who had been referred for testing. We selected ERG data, obtained using the protocol described above, from the left eye of the 22 patients who were found by us to have perfectly normal eyes, including normal acuity for age, normal alignment and motility, normal pupillary responses, normal fundi, and little or no refractive error (spherical equivalents -2 to $+4$ diopters). Their ages were 6 months to 15.1 years. Vision and ocular features have remained normal

1 to 6 years (median, 3 years) after electroretinography. None of the 22 had a family history of eye disease or visual disorders.

Growth Curve Analysis

A logistic growth curve of the form

$$y/y_{max} = \text{Age}^n / (\text{Age}^n + \text{Age}_{50}^n), \quad (3)$$

where Age_{50} is defined as the age at which y is 50% of the adults' value, y_{max} ; and the exponent, n , indicating the steepness of the curve at Age_{50} , was fit to each ERG parameter, S , R_{mp3} , V_{max} , and $1/\sigma$ (expressed as percent of the adult mean). A least squares criterion was used to determine the values that minimized the deviation of the data from Equation 3. All parameters were free to vary. The b-wave response parameters, σ and V_{max} , from an additional 71 normal subjects that we had previously studied³⁹ were included in the growth curve analysis. Also analyzed were S and R_{mp3} values reported by Nusinowitz et al.,⁴⁰ in their Figure 2, for infants and adults. In this analysis, y_{max} was fixed at the adult values of S and R_{mp3} that were reported as means.⁴⁰

TABLE 1. Scotopic ERG

A. Comparison of ERG Parameters in 10-Week-Old Infants and Children and Adults						
ERG Parameter		10-Week-Old Infants ($n = 27$)*	Children and Adults ($n = 25$)*			
a-Wave (Eq. 1)	S (scot td sec)	0.59 ± 0.19	1.20 ± 0.19			
	R_{mp3} (μV)	161 ± 51	383 ± 75			
	t_d (ms)	3.6 ± 0.7	3.4 ± 0.5			
b-Wave (Eq. 2)	Log σ (scot td sec)	-0.38 ± 0.18	-0.84 ± 0.10			
	V_{max} (μV)	194 ± 62	379 ± 59			

B. Growth Curve Parameters (Eq. 3)						
ERG Parameter	No. of Subjects	y_{max} (μV)	Age ₅₀ (weeks)†	Exponent, n	r^2	Value at 10 Weeks
S (scot td sec)	71	1.20 (1.12-1.28)	10.7 (8.9-12.5)	1.2	0.76	0.57
	93	1.17 (1.10-1.24)	10.0 (8.1-11.9)	1.4	0.66	
R_{mp3} (μV)	71	383 (357-409)	11.2 (9.4-13.0)	1.26	0.73	177
	93	388 (365-411)	11.8 (9.4-14.2)	1.26	0.68	
Log σ (scot td sec)	142	-0.85 (-0.82--0.88)	11.0 (9.3-12.7)	2.7	0.57	-0.35
V_{max} (μV)	142	384 (366-402)	10.0 (8.3-11.7)	1.2	0.68	218

* Values are means \pm SD.

† Values in parentheses are 95% CI.

For comparison to the development of the ERG parameters, the logistic growth model was applied to the development of dark-adapted, rod-mediated visual sensitivity (the reciprocal of threshold).^{3,6,8,9,27-30} These psychophysical data from 169 dark-adapted subjects had been obtained with a "fix and flash" preferential looking procedure.^{9,41} All stimuli were 50 msec in duration. Some subjects ($n = 43$) were tested with 2° diameter spots presented 10° or 30° eccentric; the youngest subject tested with these small spots was 10 weeks old.^{8,9,30} The majority ($n = 126$) were tested with 10° diameter spots presented 20° eccentric; the youngest subject tested with these large spots was 4 weeks old.^{3,6,27-29} In each stimulus condition, adults' mean threshold was designated 100%. For the growth curve analysis, sensitivity (the reciprocal of threshold) was expressed as percent of adults' mean sensitivity for the particular stimulus. For instance, a threshold that is 0.3 log unit above the mean adult threshold is 50% of the adults' mean sensitivity. Although nine infants' data had been gathered longitudinally,⁹ each sensitivity value was treated as an independent measure in the growth curve analysis. The variation in sensitivity with age was analyzed by fitting the logistic growth model to the data. For summaries of the development of rod-mediated visual sensitivity, data are also presented as log threshold, the familiar representation of visual sensitivity, and in these graphic displays, both the fitted growth curve (% sensitivity versus age) and transformed growth curve (threshold versus age) are shown.

RESULTS

Sample ERG records and model fits show all four ERG parameters, S , R_{mp3} , σ , and V_{max} , are lower in the infant than in the adult (Fig. 2). Each of the four parameters is significantly smaller (Table 1A) in 10-week-old infants (63-77 days; $n = 27$)

than in the children and adults ($n = 25$). Consistent with a previous report,⁴² there is little change in the ERG parameters between age 8 and 52 years. The ERG parameters are plotted as a function of age in Figures 3 and 4. The parameters of the logistic growth model fit to the developmental increase in each parameter are listed in Table 1B.

If logistic growth is assumed to summarize the normal developmental increase in human rod photoreceptor sensitivity, the age at which S is half the adults' mean value is 10.7 weeks (95% confidence interval [CI], 8.9-12.5 weeks) (Fig. 3A; Table 1B). Equation 3 accounts for 76% of the variation of S with age in normal subjects ($n = 71$). The age at which R_{mp3} (Fig. 3B) is half the adults' value is 11.2 weeks (95% CI, 9.4-13.0 weeks). The shape of the growth curve, as indicated by the exponent, n (Table 1B), is similar for S and R_{mp3} . The values of S and R_{mp3} at age 10 weeks, estimated by the growth curve analysis (Table 1B), agree well with the mean values at age 10 weeks (Table 1A), and values of y_{max} agree well with the mean observed values in adults (Table 1A). Inclusion of the data from the 22 patients with normal eyes in the analysis has little effect on the growth curves for S and R_{mp3} (Figs. 3A, 3B; Table 1B). The Age₅₀ values for S and R_{mp3} (Table 1B) are in reasonable agreement with those calculated for data reported by Nusinowitz et al.⁴⁰ for which Age₅₀ of S is 9.4 weeks (95% CI: 7.8-11 weeks) ($r^2 = 0.39$) and of R_{mp3} is 12.5 weeks (95% CI: 9.4-15.6 weeks) ($r^2 = 0.18$). Thus, the Age₅₀ values for the S and R_{mp3} data reported by Nusinowitz et al.⁴⁰ overlap one another and those for the subjects studied herein (Table 1B).

Assuming logistic growth describes the developmental increase in b-wave sensitivity, Age₅₀ is 11.0 weeks (95% CI, 9.3-12.7 weeks) (Fig. 4A; Table 1B). The logistic growth curve fit to saturated b-wave amplitude, V_{max} (Fig. 4B; Table 1B), reaches half of the adults' mean value at 10.0 weeks (95% CI, 8.3-11.7 weeks). The values of log σ and V_{max} estimated from the growth curve analysis at age 10 weeks are in reasonable

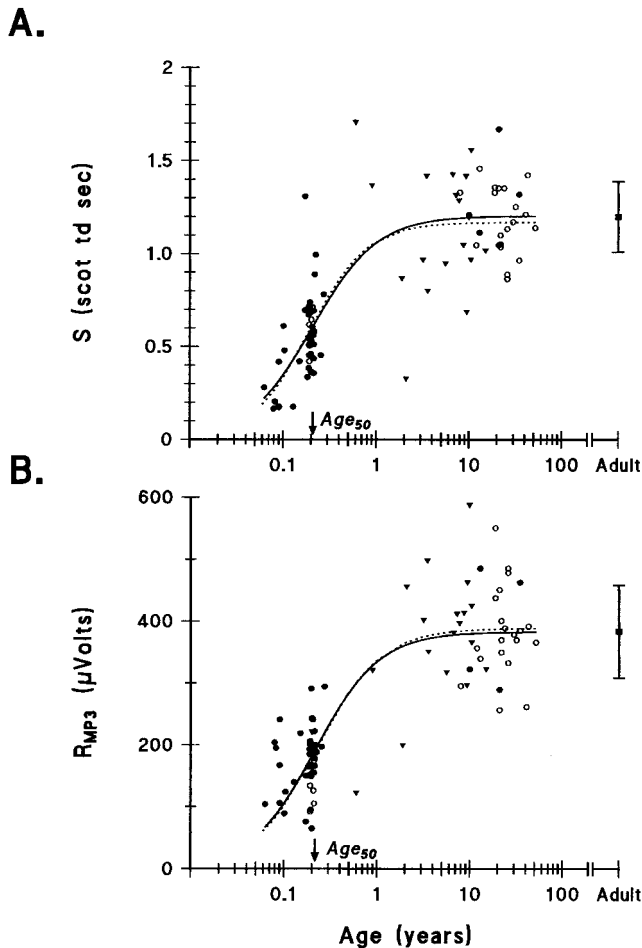


FIGURE 3. Photoreceptor response parameters (S and R_{mp3} in Eq. 1) plotted as a function of age and mean adult (\pm SD) values (*filled squares*). **(A)** Rod photoreceptor sensitivity, S . The *circles* represent the 71 main subjects in this study; the *open circles* indicate those data previously reported.^{7,38} The *solid line* is the logistic growth curve (Eq. 3) fit to the *circles*. Age_{50} is 10.7 weeks (95% CI, 8.9–12.5 weeks). See also Table 1B. The *dashed curve* is Eq. 3 fit to the *circles* and *inverted, filled triangles*, which represent the 22 patients with normal eyes. **(B)** Saturated amplitude of the rod response, R_{mp3} . The *symbols* are as in **(A)**. The *solid line* is a logistic growth curve fit to the *circles* ($n = 71$); Age_{50} is 11.2 weeks (95% CI, 9.4–13.0 weeks). See also Table 1B. The *dashed line* is the growth curve fit to the *circles* and *inverted triangles* ($n = 93$).

agreement with the observed values; y_{max} and adult means are also in reasonable agreement (Tables 1A, 1B).

The mean dark-adapted visual threshold of 10-week-old infants is significantly higher (sensitivity lower) than that of adults at all eccentricities (Table 2A); the highest infant threshold is at 10° eccentric (parafoveal). In Figure 5, for each eccentricity, the sensitivities (left) and corresponding thresholds (right)^{8,9,30} are plotted as a function of age. Assuming logistic growth of peripheral visual sensitivity (Fig. 5A, left), the calculated value of Age_{50} is 13.5 weeks (95% CI, 12.2–14.8 weeks) (Table 2B). This interval overlaps those for rod photoreceptor sensitivity, S , and b-wave sensitivity (Table 1B). By this analysis, the course of development of peripheral, dark-

adapted, rod-mediated visual sensitivity, as defined here, is concurrent with the development of rod photoreceptor (Fig. 3A) and b-wave (Fig. 4A) sensitivity.

According to the logistic growth model, the parafoveal visual threshold (Fig. 5B, right) is 0.3 log unit above (or sensitivity is half) that of an adult's threshold at 19.5 weeks (95% CI, 17.2–21.8 weeks). This is significantly older than Age_{50} for peripheral thresholds (Fig. 5A; Table 2B), and rod photoreceptor (Fig. 3A; Table 1B) or b-wave (Fig. 4A, Table 1B) sensitivity.

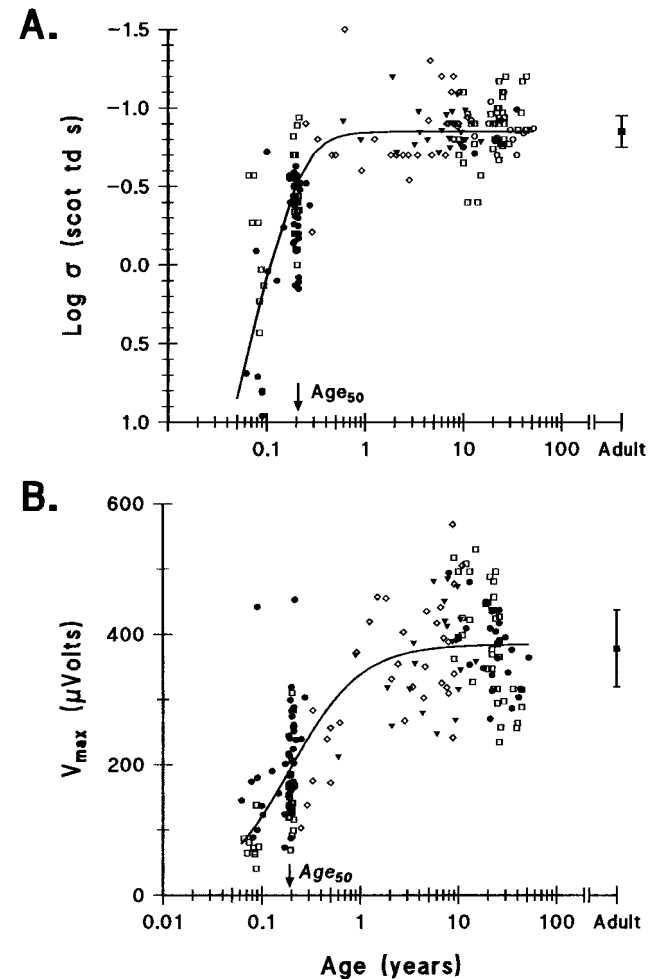


FIGURE 4. b-Wave response parameters (σ and V_{max} in Eq. 2) plotted as a function of age and mean adult (\pm SD) values (*filled squares*). In both panels, the *circles* represent normal subjects ($n = 71$), as in Figure 3, and *open squares* ($n = 71$) replot the data of normal subjects from Ref. 39. The *solid line* is Eq. 3 fit to the data from all normal subjects ($n = 142$). Also shown are the data from patients with normal eyes; the *inverted, filled triangles* are for individuals whose a-wave results are plotted in Figure 3, and the *open diamonds* are for those patients with normal eyes whose b-wave data were reported in Ref. 39. **(A)** $\text{Log } \sigma$, the flash producing a half maximum b-wave amplitude. Age_{50} for normal subjects is 11.0 weeks (95% CI, 9.3–12.7 weeks); see also Table 1B. Note that this is a log-log display, with the rising limb linear, rather than S-shaped, as in the linear-log display shown in **(B)**. **(B)** Saturated b-wave amplitude, V_{max} . Age_{50} for normal subjects is 10.0 weeks (95% CI, 8.3–11.7 weeks); see also Table 1B.

TABLE 2. Dark Adapted Scotopic Visual Thresholds

Stimuli, 50-msec Duration		A. Comparison of Thresholds in 10-Week-Old Infants and Adults					
Diameter	Eccentricity	Mean Thresholds (log scot td sec)*		Infant-Adult Difference			
		10-Week-Old Infants	Adults	Log Unit	t-Value	df	P
2°	30°	-2.65 ± 0.15 (25)	-3.21 ± 0.14 (18)	0.56	12.16	41	<0.01
2°	10°	-2.15 ± 0.16 (25)	-3.21 ± 0.13 (18)	1.06	23.27	41	<0.01
10°	20°	-2.68 ± 0.27 (68)	-3.90 ± 0.12 (26)	1.22	22.3	92	<0.01

Stimuli, 50-msec Duration		B. Growth Curve Parameters (Eq. 3)						
Diameter	Eccentricity	No. of Thresholds	y _{max} (%)	Age ₅₀ (weeks)†	Exponent, n	r ²	Threshold at 10 Weeks (log scot td sec)	
2°	30°	62	100	13.5 (12.2-14.8)	2.7	0.66	-2.68	
2°	10°	62	100	19.5 (17.2-21.8)	2.7	0.78	-2.36	
10°	20°	126	100	33.0 (26.2-39.8)	2.9	0.85	-2.36	

* Values in parentheses are number of subjects.

† Values in parentheses are 95% CI.

In Figure 5C (right), the dark-adapted, rod-mediated thresholds for detection of large, 10° diameter spots, presented 20° eccentric, are shown. According to the logistic growth curve, the age at which the threshold is 0.3 log unit above (or sensitivity is half) that of an adult's, is 33.0 weeks (95% CI, 26.2-39.8 weeks).

DISCUSSION

The developmental courses of rod photoreceptor sensitivity, b-wave sensitivity, and peripheral rod-mediated visual sensitivity are statistically indistinguishable. Even though the ERG and psychophysical data were not gathered following a within-subject design, the 95% CIs overlap for the ages at which rod photoreceptor, b-wave, and peripheral visual sensitivity reach half the adult's value (Fig. 6). Additionally, the shape of the summarizing growth curves, defined by the exponent *n*, is similar (Tables 1B, 2B). The developmental course for visual sensitivity mediated by parafoveal retina is relatively delayed, as is rod outer segment maturation in the parafoveal region.^{10,14} Sensitivity measured with large (10° diameter) spots centered at the rod ring¹⁴ is also relatively delayed. In infants, the large spots must test retina-containing rod outer segments in various states of maturation.^{10,14}

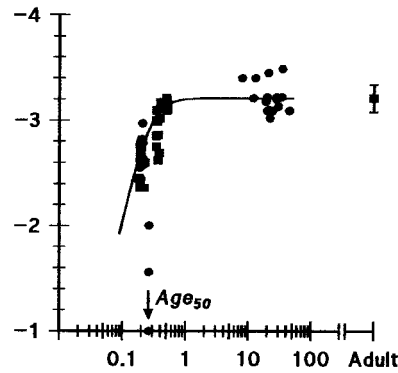
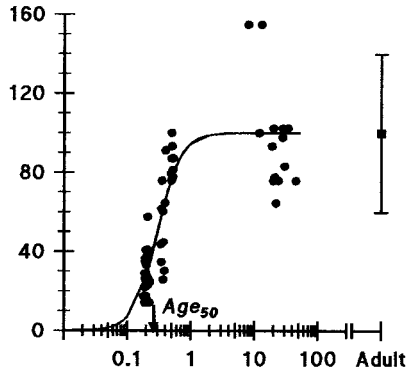
In developing rat retina, it has been possible to demonstrate that the developmental increase in rhodopsin content, rod photoreceptor, and b-wave sensitivity follow the same course. There is not broad overlap of the course of development of human rhodopsin and rod photoreceptor sensitivity (Fig. 6). As the large confidence interval for human rhodopsin indicates, the content of rhodopsin in human eyes is quite variable.¹⁵ The variability is due not only to bleaching, but also likely depends on numbers of rods per retina and perhaps on long-term adaptations to ambient light.^{15,22}

The logistic growth curve has been fit empirically to the data herein. In other species, this model provides a satisfactory summary of developmental increases in rhodopsin (as shown, e.g., in Fig. 1) and other proteins involved in phototransduction processes as well as growth of outer segment length.^{11,19,22} Furthermore, in developing rats, the amount of rhodopsin available for capture of light and the numbers of channels in the outer segment membranes available for closure by light are proportional to the rod photoreceptor response parameters, *S* and *R_{mp3}*.^{11,43} In other words, during development, rod photoreceptor sensitivity is scaled by the amount of rhodopsin present, and the amount of rhodopsin present is proportional to the number of channels in the receptor membrane that are available for closure by light. As the present data for human development show, the rat b-wave response parameters, perhaps representing mainly the on-bipolar cells,^{26,36} which take their input from the rods, have the same developmental course as the rod photoreceptor response parameters.¹¹

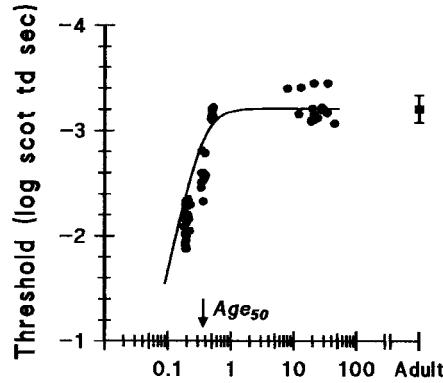
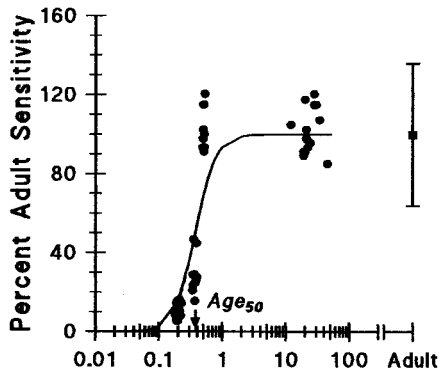
Immaturities of rod-mediated, human retinal function may depend on similar rod outer segment immaturities, although the anatomic data are sparse.^{8-10,14} Infants' higher visual thresholds at parafoveal than peripheral sites were reasoned to be consistent with shorter parafoveal rod outer segments.⁸ The courses of maturation of the visual thresholds at parafoveal and peripheral sites appear to be a consequence of a later course of maturation of the parafoveal than peripheral rod outer segments.⁹

Other results are also consistent with rods as the main determinant of 10-week-old infants' lower scotopic visual sensitivity. Sensitivities derived from scotopic ERG and VEP responses to full-field stimuli were examined.⁴ The differences between infants' and adults' rod (ERG a-wave), inner retinal (ERG b-wave), and VEP sensitivities were all the same,⁴ and, in fact, similar to the infant-adult difference

A. Peripheral (30° Eccentric)



B. Parafoveal (10° Eccentric)



C. Rod Ring (20° Eccentric)

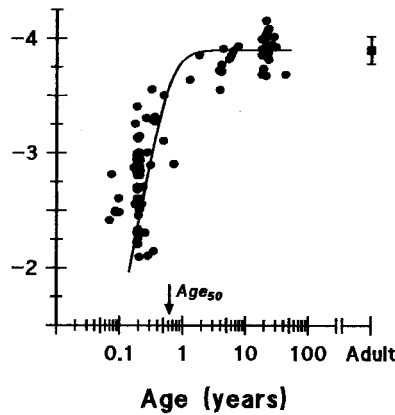
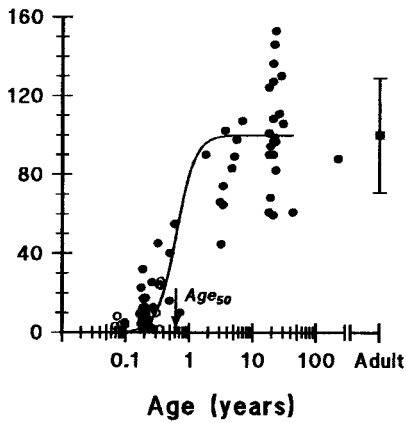


FIGURE 5. For stimuli at 30°, 10° (parafoveal), and 20° eccentric in (A), (B), and (C), respectively, the dark-adapted visual sensitivity (left) or threshold (right) is shown as a function of age. On the left, the smooth curve is the logistic growth model fit to the data expressed as percent of adults' mean sensitivity and displayed on log-linear coordinates. On the right, the data are plotted as log threshold, and the fitted growth curve is transformed for the log-log displays. In each panel, the square and error bars indicate the mean \pm SD value in adults.

subsequently found for peripheral visual sensitivity at age 10 weeks,⁴ namely approximately 0.5 log unit. Thus, it seemed likely that the determination of 10-week-old infants' scotopic, dark-adapted visual sensitivity was primarily in the rods.

The present study evaluates sensitivity from early infancy through middle age. The concurrent courses of development of rod sensitivity, b-wave sensitivity, and peripheral visual sensitivity suggest that the maturation of the rod outer segments

and quantum catch govern the developmental increase in dark-adapted scotopic visual sensitivity. Although recognizing the influence of receptive field immaturities on infants' scotopic visual responses,^{2,29,41,44} the data herein as well as the results of analysis of the *eigengrau* in infants' parafoveal and peripheral retina⁴⁵ are evidence that rod outer segment immaturities, with consequent low probability of quantum capture, are critical determinants of dark-adapted infants' low scotopic visual sensitivity.

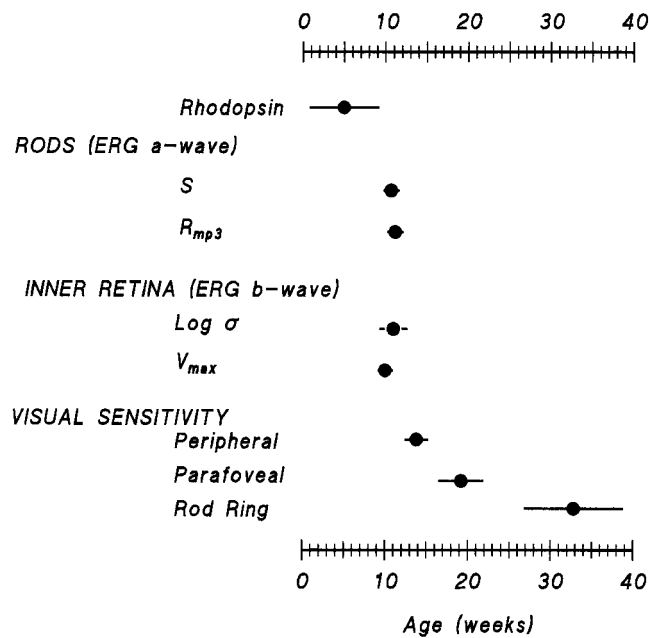


FIGURE 6. Summary of developmental courses of rhodopsin, retinal and visual sensitivity. The results of the growth curve analyses presented in Figures 3, 4, and 5 are shown as the Age₅₀ values along with the 95% CIs. Also shown is the Age₅₀ value, 5 weeks (95% CI, 0-10 weeks), reported for human rhodopsin.¹⁵ The CIs for rhodopsin and the ERG and peripheral visual sensitivity parameters overlap.

References

- Brown AM. Scotopic sensitivity of the two-month-old human infant. *Vision Res.* 1986;26:707-711.
- Hamer RD, Schneck ME. Spatial summation in dark-adapted human infants. *Vision Res.* 1984;24:77-85.
- Hansen RM, Fulton AB, Harris SJ. Background adaptation in human infants. *Vision Res.* 1986;26:771-779.
- Hansen RM, Fulton AB. The VEP thresholds for full-field stimuli in dark adapted 10-week old infants. *Vis Neurosci.* 1995;12:223-228.
- Powers MK, Schneck ME, Teller DY. Spectral sensitivity of human infants at absolute visual threshold. *Vision Res.* 1981;21:1005-1016.
- Hansen RM, Fulton AB. Development of scotopic retinal sensitivity. In: Simons K, ed. *Early Visual Development, Normal and Abnormal.* New York: Oxford University Press; 1993:130-142.
- Fulton AB, Hansen RM. The rod sensitivity of dark adapted human infants. *Curr Eye Res.* 1992;11:1193-1198.
- Hansen RM, Fulton AB. Dark adapted thresholds at 10 deg and 30 deg eccentricities in 10-week old infants. *Visual Neurosci.* 1995;12:509-512.
- Hansen RM, Fulton A. The course of maturation of rod mediated visual thresholds in infants. *Invest Ophthalmol Vis Sci.* 1999;40:1883-1885.
- Hendrickson AE, Drucker D. The development of parafoveal and midperipheral retina. *Behav Brain Res.* 1992;19:21-32.
- Fulton AB, Hansen RM, Findl O. The development of the rod photoreponse from dark adapted rats. *Invest Ophthalmol Vis Sci.* 1995;36:1038-1045.
- Brown AM. Development of visual sensitivity to light and color in human infants: a critical review. *Vision Res.* 1990;30:1159-1188.
- Hood DC. Testing hypotheses about development with electroretinographic and increment threshold data. *J Optical Soc Am (A).* 1988;5:2159-2165.
- Hendrickson AE. The morphologic development of human and monkey retina. In: Albert DM, Jakobiec FA, eds. *Principles and*

Practice of Ophthalmology: Basic Sciences. Philadelphia: WB Saunders; 1994:561-577.

- Fulton AB, Dodge J, Hansen RM, Williams TP. The rhodopsin content of human eyes. *Invest Ophthalmol Vis Sci.* 1999;40:1878-1883.
- Bonting SL, Caravaggio LL, Gouras P. The rhodopsin cycle in the developing vertebrate retina: I. Relation of rhodopsin content, electroretinogram and rod structure in the rat. *Exp Eye Res.* 1961;1:14-24.
- Fulton AB, Hansen RM, Dorn E, Hendrickson AE. Development of primate rod structure and function. In: Vital-Durand F, Atkinson J, Braddock OJ, eds. *Infant Vision.* Oxford: Oxford University Press; 1996:33-49.
- LaVail M. Kinetics of rod outer segment renewal in the developing mouse retina. *J Cell Biol.* 1973;58:650-661.
- Timmers AM, Fox D, He L, Hansen RM, Fulton AB. Rod photoreceptor maturation does not vary with retinal eccentricity in mammalian retina. *Curr Eye Res.* 1999;18:393-402.
- Hoglund G, Nilsson SE, Schwemer J. Visual pigment and visual receptor cells in adult sheep. *Invest Ophthalmol Vis Sci.* 1982;23:409-418.
- Fulton AB, Dodge J, Hansen RM, Schremser J-L, Williams TP. The quantity of rhodopsin in young human eyes. *Curr Eye Res.* 1991;10:977-982.
- Fulton A, Hansen R, Dodge J, Williams T. Photoreceptor development and photostasis. In: Williams TP, Thistle A, eds. *Photostasis and Related Phenomena.* New York: Plenum Press; 1998:189-198.
- Snedecor GW, Cochran WG. *Statistical Methods,* 7th ed. Ames: Iowa State University Press; 1980.
- Hood DC, Birch DG. Rod phototransduction in retinitis pigmentosa: Estimation and interpretation of parameters derived from the rod a-wave. *Invest Ophthalmol Vis Sci.* 1994;35:2948-2961.
- Lamb TD, Pugh EN Jr. A quantitative account of the activation steps involved in phototransduction in amphibian photoreceptors. *J Physiol.* 1992;449:719-758.
- Robson J, Frishman L. Response linearity and kinetics of the cat retina: the bipolar cell component of the dark-adapted electroretinogram. *Vis Neurosci.* 1995;12:837-850.
- Fulton AB, Hansen RM, Yeh Y-L, Tyler CW. Temporal summation in dark adapted 10-week-old infants. *Vision Res.* 1991;31:1259-1269.
- Hansen RM, Fulton AB. Scotopic optokinetic nystagmus (OKN) thresholds in 10 week old infants. *Invest Ophthalmol Vis Sci.* 1994;35:1246-1249.
- Hansen RM, Hamer RD, Fulton AB. The effect of light adaptation on scotopic spatial summation in 10-week-old infants. *Vision Res.* 1992;32:387-392.
- Reisner DS, Hansen RM, Findl O, Petersen RA, Fulton AB. Dark adapted thresholds in children with histories of mild retinopathy of prematurity. *Invest Ophthalmol Vis Sci.* 1997;38:1175-1183.
- Birch DG, Fish GE. Rod ERGs in retinitis pigmentosa and cone-rod degeneration. *Invest Ophthalmol Vis Sci.* 1987;28:140-150.
- Wyszecki G, Stiles WS. *Color Science: Concepts and Methods, Quantitative Data and Formulae.* New York: John Wiley & Sons; 1982:102-103.
- Larsen J. The sagittal growth of the eye. I. Ultrasonic measurement of the depth of the anterior chamber from birth to puberty. *Acta Ophthalmol.* 1971;49:239-262.
- Kraft TW, Schneeweis DM, Schnapf JL. Visual transduction in human rod photoreceptors. *J Physiol.* 1993;464:747-765.
- Pugh EN, Jr, Lamb TD. Amplification and kinetics of the activation steps in phototransduction. *Biochim Biophys Acta.* 1993;1141:111-149.
- Robson JG, Frishman IJ. Dissecting the dark adapted electroretinogram. *Doc Ophthalmol.* 1999;95:187-215.
- Peachey NS, Alexander KR, Fishman GA. The luminance-response function of the dark-adapted human electroretinogram. *Vision Res.* 1989;29:263-270.

38. Jiang C, Hansen RM, Gee B, Kurth SS, Fulton AB. Rod and rod mediated function in patients with beta thalassemia major. *Doc Ophthalmol*. 1999;96:333-346.
39. Fulton AB, Hansen RM. Workup of the possibly blind child. In: Isenberg SJ, ed. *The Eye in Infancy*. St. Louis: Mosby; 1994:547-560.
40. Nusinowitz S, Birch DG, Birch EE. Rod photoresponses in 6-week and 4-month old human infants. *Vision Res*. 1998;38:627-635.
41. Schneck ME, Hamer RD, Packer OS, Teller DY. Area threshold relations at controlled retinal locations in 1-month-old human infants. *Vision Res*. 1984;24:1753-1763.
42. Birch DG, Anderson JL. Standardized full-field electroretinography: Normal values and their variation with age. *Arch Ophthalmol*. 1992;110:1571-1576.
43. Dodge J, Fulton AB, Parker C, Hansen RM, Williams TP. Rhodopsin in immature rod outer segments. *Invest Ophthalmol Vis Sci*. 1996;37:1951-1956.
44. Hansen RM, Fulton AB. Scotopic center surround organization in 10-week-old infants. *Vision Res*. 1994;34:621-624.
45. Hansen RM, Fulton AB. Scotopic increment thresholds at parafoveal and peripheral retinal sites in young infants [ARVO Abstract]. *Invest Ophthalmol Vis Sci*. 1999;40(4):S410. Abstract nr 2159.